J|A|C|S
ARTICLES
Published on Web 10/22/2002

Self-Assembled M_6L_4-Type Coordination Nanocage with 2,2′-Bipyridine Ancillary Ligands. Facile Crystallization and X-ray Analysis of Shape-Selective Enclathration of Neutral Guests in the Cage

Takahiro Kusukawa and Makoto Fujita*

Contribution from Department of Applied Chemistry School of Engineering, The University of Tokyo and CREST, Japan Science and Technology Corporation (JST), Tokyo, Bunkyo-ku, Tokyo 113-8656, Japan

Received May 20, 2002

Abstract: Hollow and roughly spherical cage **1** (ca. 2 nm in diameter) is self-assembled from 2,4,6-tri(4-pyridyl)-1,3,5-triazine (**2**) and Pd(diamine)$(ONO_2)_2$ (**3**). This cage compound enclathrates a variety of neutral organic molecules in an aqueous phase. Unlike cage **1a**, which possesses ancillary ethylenediamine ligands on the metal centers, 2,2′-bipyridine(bipy)-protected cage **1b** is easily crystallized, making possible the detailed analysis of the enclathration geometry of guests by X-ray crystallographic study. It is found that guests are enclathrated in three different manners, depending upon the shape and the size of the guests: tetrahedral 1:4 complexation, orthogonal 1:2 complexation, and a simple 1:1 complexation. The solution structures elucidated by NMR are in good accordance with the solid structure, showing that the enclathration geometries in the solid state are kept even in solution.

Introduction

Recent development in noncovalent synthesis has made possible the facile preparation of large, hollow cage frameworks, which can hardly be synthesized by conventional synthetic methods. Consequently, host−guest chemistry with 3D hosts[1] is revived, as big molecules or molecular *aggregates* can be targeted as a new family of guests. One of the most attractive features in enclathrating molecular aggregates is the discovery of new physical and chemical properties of molecules due to aggregate formation in the restricted micro environment of the cages.[2] To develop such new properties, the inclusion geometry of the molecules in the cage must be well designed and precisely analyzed. In previous examples, however, the inclusion geometry of guests has been, in most cases, discussed on the basis of NMR in solution. Although more details can be analyzed by X-ray studies, difficulties are often encountered in crystallizing large inclusion complexes.[3,4]

Recently, coordination cage **1a**, which assembles from six metal ions and four ligands,[5a] has been shown to strongly bind a variety of neutral guests in their aggregated forms: from small aromatic guests such as benzene to large hydrophobic molecules such as *o*-carborane and adamantane derivatives.[5b,5c] Spectroscopic study suggests that there are three-types of inclusion geometries, depending upon the shape and the size of guest molecules, as shown in Chart 1. (i) When a guest dimension is smaller than the portal size (ca 8 Å in diameter), a 1:4 host−guest complex is formed, four guest molecules being aggregated along the tetrahedral axes of the complex, examples of which include substituted benzenes, adamantane, and *o*-carborane. (ii) Medium-sized, bending molecules such as diphenylmethane and *cis*-stilbene prefer to orthogonally dimerize into spherical aggregates. (iii) Large guest molecules with the dimension of >8 Å, such as tri-*tert*-butylbenzene, form 1:1 complex. These inclusion manners have been elucidated by spectroscopic methods. However, reliable X-ray analysis has not been carried out because the attempts to prepare single crystals of the complexes have been unsuccessful. Previously, we reported on the crystal structure of **1a** accommodating an anionic guest

* To whom correspondence should be addressed. E-mail: mfujita@appchem.t.u-tokyo.ac.jp.

(1) Cram D. J.; Cram J. M. *Container Molecules and Their Guests*; RSC: Cambridge, United Kingdom, 1994.
(2) Stabilization and activation of molecules enclathrated in the cavity: (a) Cram, D. J.; Tanner, M. E.; Thomas, R. *Angew. Chem., Int. Ed. Engl.* **1991**, *30*, 1024. (b) Warmuth, R. *Angew. Chem., Int. Ed. Engl.* **1997**, *36*, 1347. (c) Warmuth, R. *J. Chem. Soc. Chem. Commun.* **1998**, 59. (d) Warmuth, R.; Marvel, M. A. *Angew. Chem., Int. Ed. Engl.* **2000**, *39*, 1117. (e) Kang, J.; Santamaría, J.; Hilmersson, G.; Rebek, J., Jr. *J. Am. Chem. Soc.* **1998**, *120*, 7389. (f) Kang, J.; Rebek, J., Jr. *Nature* **1996**, *382*, 239. (g) Kang, J.; Hilmersson, G.; Santamaría, J.; Rebek, J., Jr. *J. Am. Chem. Soc.* **1998**, *120*, 3650. (h) Ziegler, M.; Brumaghim, J. L.; Raymond, K. N.; *Angew. Chem., Int. Ed. Engl.* **2000**, *39*, 4119.
(3) (a) Timmerman, P.; Verboom, W.; van Veggel, F. C. J. M.; van Duynhoven, J. P. M.; Reinhoudt, D. N. *Angew. Chem., Int. Ed. Engl.* **1994**, *33*, 2345. (b) van Wageningen, A. M. A.; Timmerman, P.; van Duynhoven, J. P. M.; Verboom, W.; van Veggel, F. C. M.; Reinhoudt, D. N. *Chem. Eur. J.* **1997**, *3*, 639. (c) Fraser, J. R.; Borecka, B.; Trotter, J.; Sherman, J. C. *J. Org. Chem.* **1995**, *60*, 1207. (d) Sherman, J. C.; Knobler, C. B.; Cram, D. J. *J. Am. Chem. Soc.* **1991**, *113*, 2194. (e) Chapman, R. G.; Sherman, J. C. *J. Org. Chem.* **2000**, *65*, 513. (f) Naumann, C.; Place, S.; Sherman, J. C. *J. Am. Chem. Soc.* **2002**, *124*, 16.
(4) (a) Heinz, T.; Rudkevich, D. M.; Rebek, J., Jr. *Nature* **1998**, *394*, 764. (b) Heinz, T.; Rudkevich, D. M.; Rebek, J., Jr. *Angew. Chem., Int. Ed.* **1999**, *38*, 1136. (c) Ma, S.; Rudkevich, D. M.; Rebek, J., Jr. *Angew. Chem., Int. Ed.* **1999**, *38*, 2600. (d) Tucci, F. C.; Rudkevich, D. M.; Rebek, J., Jr. *J. Am. Chem. Soc.* **1999**, *121*, 4928.
(5) (a) Fujita, M.; Oguro, D.; Miyazawa, M.; Oka, H.; Yamaguchi, K.; Ogura, K. *Nature* **1995**, *378*, 469. (b) Kusukawa, T.; Fujita, M. *Angew. Chem., Int. Ed. Engl.* **1998**, *37*, 3144. (c) Kusukawa, T.; Fujita, M. *J. Am. Chem. Soc.* **1999**, *121*, 1397.

10.1021/ja020712k CCC: $22.00

Chart 1

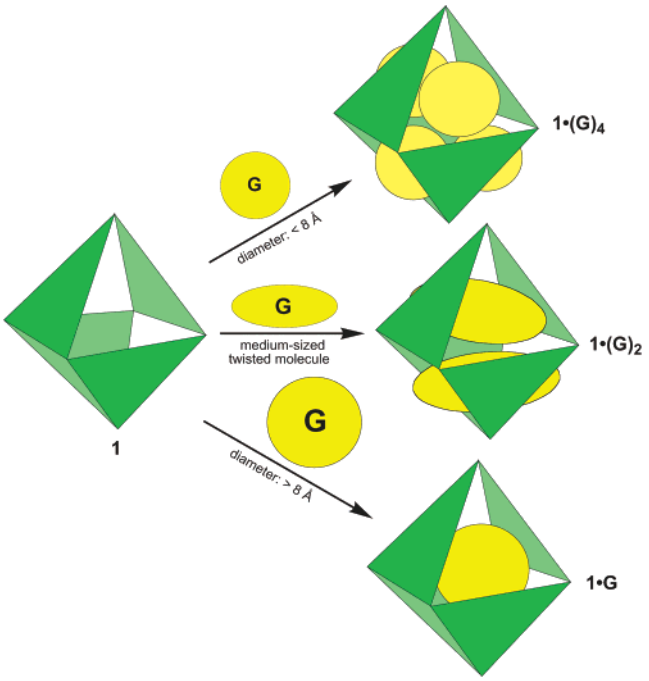

molecule (adamantanecarboxylate), where cation−anion interactions contribute to the host−guest complexation.[5a] However, the complexes of **1a** with neutral guests have never been analyzed by X-ray diffraction. To improve the crystallinity of the cage complex, the ancillary ethylenediamine ligand on the Pd(II) centers is replaced by more rigid 2,2′-bipyridine (bipy). We have found that the inclusion complexes of **1b** are much more easily crystallized than those of **1a** and succeeded in the X-ray crystallographic analysis of the above-mentioned, three different inclusion geometries. Accordingly, we discuss here the crystal structures of cage **1b** with neutral guest molecules. The solid structures thus obtained are in good accordance with solution structures elucidated by NMR, showing that the enclathration geometry in the solid-state remains unchanged even in solution.

Results and Discussion

Synthesis of Cage 1b. Coordination cage **1b** was synthesized according to the reported procedure for the preparation of **1a** (Scheme 1). Ligand **2** was suspended in an H_2O−MeOH solution of **3b**, and the mixture was heated to 80 °C. After 30 min, a pale yellow clear solution was obtained. Analysis of the solution by NMR spectroscopy showed the quantitative self-assembly of **1b**. Condensation of the solution precipitated pure **1b** as a pale yellow powder in 70% yield. The elemental analysis agreed with the empirical formulas of **1b**·$9H_2O$. Due to the high symmetry of the cage (T_d symmetry), the twelve pyridine rings in **1b** are all equivalent, and the NMR spectrum of **1b** displays only a set of pyridine protons at δ = 9.47 (PyH^{α}) and 8.92 (PyH^{β}) for the ligand **2** moiety.

Enclathration of Spherical Guest Molecules: 1:4 Complexation. *o*-Carborane. Previously, the remarkable ability of **1a** for enclathrating large molecules was demonstrated by the inclusion of as many as four molecules of *o*-carborane (**4**), a spherical molecule with a diameter of 8 Å.[5b] Cage **1b** also bound **4** to give the same 1:4 complex. The complexation was easily

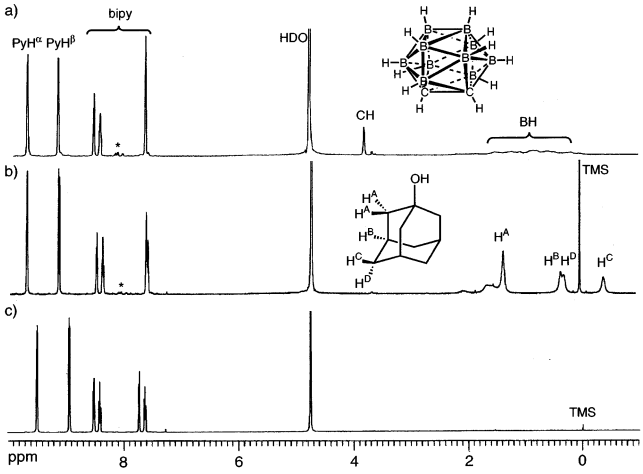

Figure 1. ^{1}H NMR observations of the enclathration of guest molecules in **1b**. (a) **1b**·(**4**)$_4$. (b) **1b**·(**5**)$_4$. (c) Empty **1b** (∗: impurities).

Scheme 1

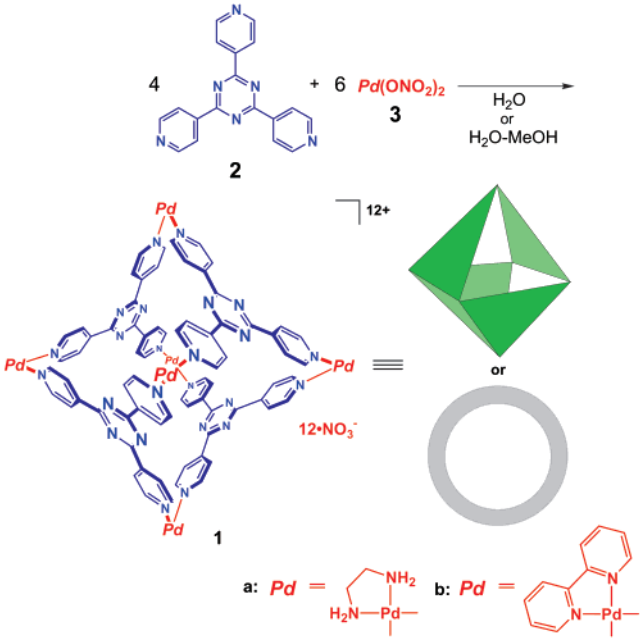

accomplished by simply mixing a hexane solution of **4** (4.5 equiv) with a D_2O solution of **1b**. Within 30 min at room temperature, 4 equiv of **4** were efficiently transferred into the aqueous phase to give **1b**·(**4**)$_4$, as monitored by ^{1}H NMR (Figure 1a). The B*H* signals of **4** appear at δ 1.7 ≈ 0.0 (Figure 1a) due to the enclathration of **4** in cage **1b**. The 1:4 stoichiometry was confirmed by the integral ratio of **1b** and **4** in ^{1}H NMR. The aqueous solution was condensed to precipitate enclathrated complex **1b**·(**4**)$_4$ as a pure, pale yellow powder in 84% yield. The stoichiometry of **1b**·(**4**)$_4$·$(H_2O)_4$ was shown by elemental analysis.

The use of bipy as the end-capped ligand on Pd centers was quite effective for the crystallization of the enclathration complex. Thus, unlike the **1a**·(**4**)$_4$ complex, which has been never crystallized, **1b**·(**4**)$_4$ was easily crystallized by allowing its aqueous solution to stand at room temperature for a few days. The crystal structure of **1b**·(**4**)$_4$ showed that four guest molecules form (**4**)$_4$ aggregates in the cavity, with their main axes being pointed to the corners of a tetrahedron (Figure 2). Though the diffraction data were collected at −150 °C, nitrate ions and water

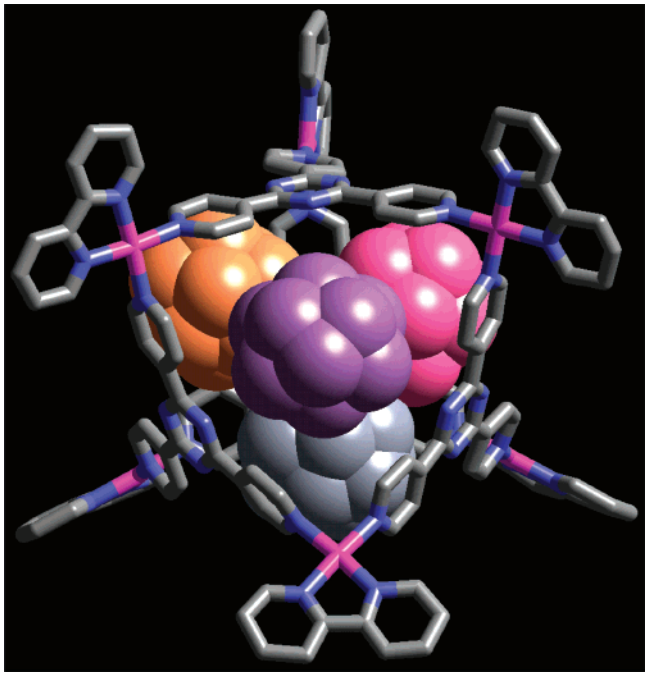

Figure 2. Crystal structure of **1b**·(**4**)$_4$.

molecules were partially disordered and not fully located. Spherical guest **4** seems to spin even at low-temperature, making it difficult to distinguish carbon from boron atoms in the crystallographic analysis.

The orientation of the guests was rather elucidated from ^{1}H NMR study. B*H* signals of **4** were significantly upfield shifted, whereas C*H* signals were much less shifted, suggesting that guest molecule **4** is oriented in such a way that negative (B*H*)$_n$ part is pointed inward while positive C*H* is outward.

1-Adamantanol (5). This spherical molecule (ca. 6 Å in diameter) was also efficiently enclathrated by **1b** in a 1:4 ratio. Typically, **1b**·(**5**)$_4$ complexes were formed by treating a saturated hexane solution of **5** with D_2O solution of **1b** at 60∼80 °C for 30 min (Figure 1b). Single crystals were easily grown by allowing the aqueous solution of **1b**·(**5**)$_4$ to stand at room temperature for a few days. The crystal structure of **1b**·(**5**)$_4$ showed that four guest molecules were efficiently enclathrated in the cavity of **1b** in a manner similar to the **1b**·(**4**)$_4$ formation (Figure 3). Despite the absence of strong host−guest interactions, guest molecules **5** are not disordered but located at a fixed geometry; that is, hydrophobic adamantyl groups are located inside, whereas hydrophilic hydroxyl groups are located outside.

The guest geometry determined by X-ray analysis was consistent with the spectroscopic observation of the solution structure. In ^{1}H NMR, the upfield shift ($\Delta\delta$) of guest signals ranges from −0.4 to −2.1 ppm; some protons are shifted significantly but others are not (Figures 1b and 4). This implies that the guest geometry is fixed even in solution. The assignment of all protons H^A−H^D, based on 2D-NMR analysis, made it clear that protons away from the OH group are significantly shifted, whereas those close to the OH group are not (Figure 4). This result shows that the interior of host **1b** is highly hydrophobic, and the guest molecule is located in the cage in the same way as observed by X-ray analysis.

Enclathration of Medium, Bending Molecules: 1:2 Complexation. Previously, we reported that the remarkable ability

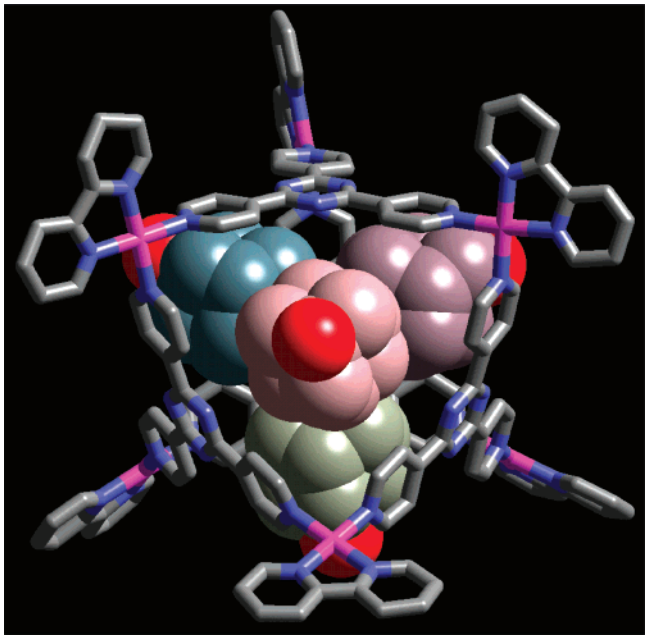

Figure 3. Crystal structure of **1b**·(**5**)$_4$.

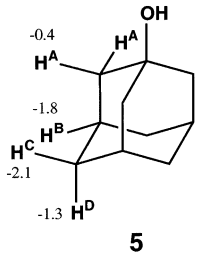

5

Figure 4. Change in the NMR chemical shifts of adamantanol guest **5** upon inclusion in **1b**. Negative values indicate upfield shift values ($\Delta\delta$ in ppm).

of cage **1a** for the selective enclathration of medium-sized bending molecules such as *cis*-azobenzene and -stilbene derivatives.[5c] These guest molecules are enclathrated in the cavity through the "ship-in-a-bottle" formation of a hydrophobically interacted dimer, where *cis*-azobenzene was considerably stabilized and did not isomerize to its *trans*-isomer. Interestingly, *trans*-stillbene and -azobenzene were not enclathrated because these rodlike molecules have no chance of fitting into the spherical cavity of cage **1a** in any of its aggregation forms. Thus, the bending shape is essential to aggregate into a spherical dimer. The structure of the hydrophobic dimer has been speculated from MD simulation but not evidenced by a convincing crystallographic analysis.[5c] To obtain the crystal structure of the hydrophobic dimer, we again employed **1b**, instead of **1a**, as the host. The crystals suitable for X-ray analysis were obtained when diphenylmethane (**6**) and 4,4′-dimethoxybenzoyl (**7a**) were examined as guests (Schemes 2 and 3).[6]

Diphenylmethane. Conformationally flexible diphenylmethane (**6**) was also enclathrated by **1b** in a 1:2 ratio. A D_2O solution of **1b** was stirred with a saturated hexane solution of **6** at 80 °C and single crystals were grown by allowing an aqueous solution of **1**·(**6**)$_2$ to stand at room temperature. The crystal structure of **1b**·(**6**)$_2$ showed that two guest molecules are enclathrated orthogonally inside the nanosized cavity of **1b**

(6) Preliminary results were communicated in: Kusukawa, T.; Yoshizawa, M.; Fujita, M. *Angew. Chem., Int. Ed.* **2001**, *40*, 1879.

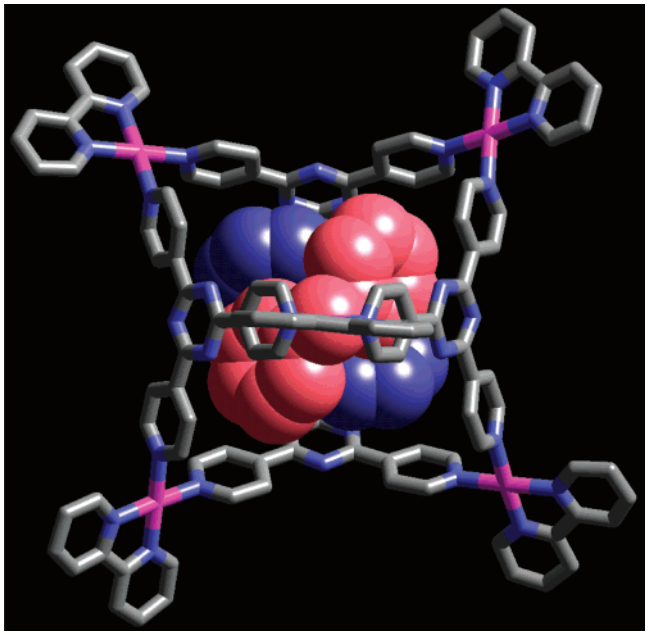

Figure 5. Crystal structure of **1b**·(**6**)$_4$.

Scheme 2

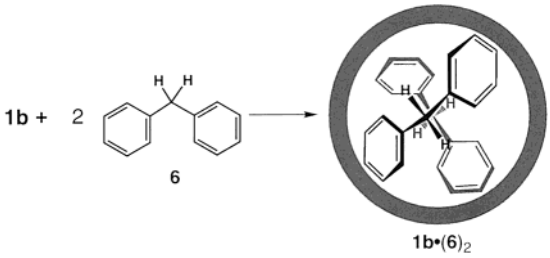

Scheme 3

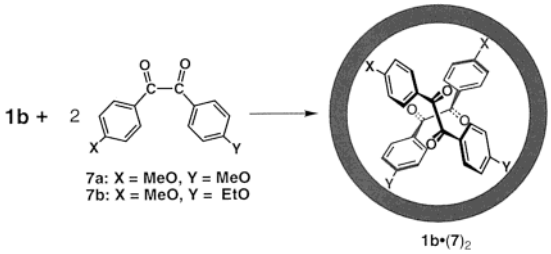

(Figure 5). Efficient CH−π and π−π interactions (~3.3−3.6 Å) between two aromatic rings of **6** were observed, showing the importance of intermolecular CH−π interactions for the hydrophobic dimer formation. This result strongly implies that the related twisted molecules, such as *cis*-azobenzene and -stilbene, which also from stable 1:2 complexes, adopt a similar dimeric structure in the cavity of **1a**.

1,2-Bis(4-methoxypheny)-1,2-ethanedione. This 1,2-diketone molecule can also adopt a bending conformation when two carbonyls are twisted to some extent. Because the twisted conformation is chiral, we may consider dl/meso isomers for the hydrophobic dimer. The spectroscopic observation showed the formation of a stable 1:2 inclusion complex **1b**·(**7a**)$_2$ in which a meso-hydrophilic dimer was selectively formed. As we have already discussed,[6] the meso-dimeric structure has been proven by the symmetric analysis of the **1b**·(**7a**)$_2$ complex. Namely, the meso dimer should adopt S_4 symmetry, which decreases the symmetry of the cage from T_d to S_4 through host−

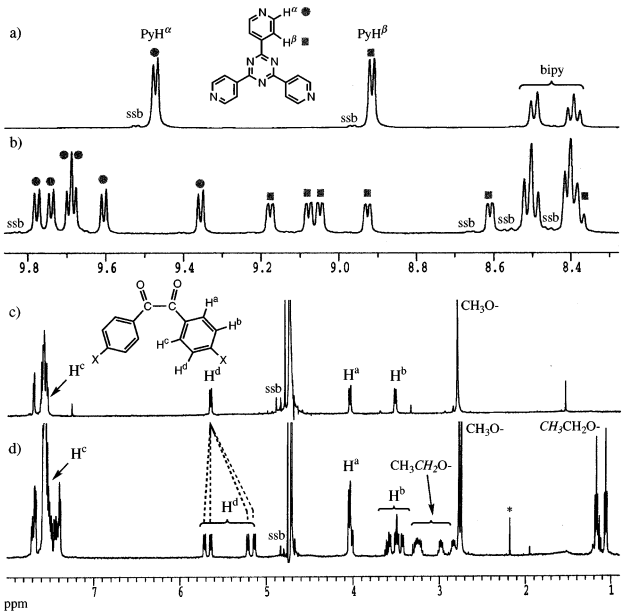

Figure 6. NMR observations of the enclathration of **7** in nanocage **1b** (a) empty **1b**, (b) and c) **1b**·(**7a**)$_2$ complex, (d) **1b**·(**7b**)$_2$ complex (*, impurity; ssb, spinning sideband).

guest interaction. Accordingly, pyridine protons of the host were split into six pairs: six PyH^α protons at δ 9.35−9.8 and six PyH^β protons at δ 8.35−9.2 (Figure 6b). This observation suggested the desymmetrization of the host into an S_4 symmetric entity with 12 inequvalent protons on each ligand. The S_4 orientation of the guests was also supported by the guest signals. The twisted conformation of **7a** was consistent with the observation of four aromatic protons of each phenylene group at different chemical shifts (Figure 6c). The observation of the chirality for each guest demonstrated that the conformation of enclathrated **7a** was completely frozen at room temperature, though that of free **7a** is not fixed in solution. With ethoxy methoxy substituted analogue **7b**, each proton of **7b** is split into a 1:1 pair of two signals because two molecules are placed in a diastereotopic environment when dimerized (e.g., see two signals at 2.78 and 2.81 ppm for the MeO groups, in Figure 6d).[7]

The proposed orientation of **7a** was finally confirmed by an X-ray analysis (Figure 7). As expected, two molecules were

(7) In (**7a**)$_2$, part A is inequivalent with A′. Note that the carbonyl of A is pointed toward A′, whereas that of A′ is toward B. Hence two molecules are inequivalent.

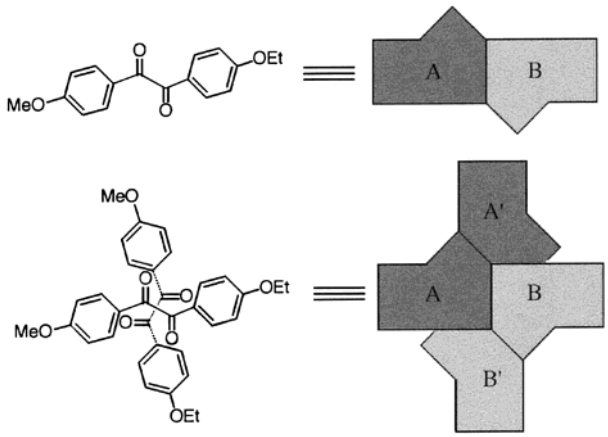

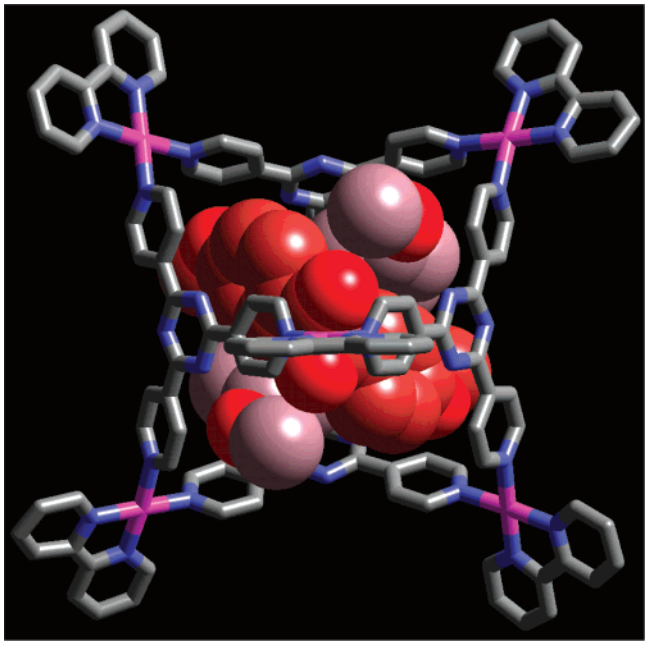

Figure 7. Crystal structure of **1b**·(**7a**)$_2$.

Scheme 4

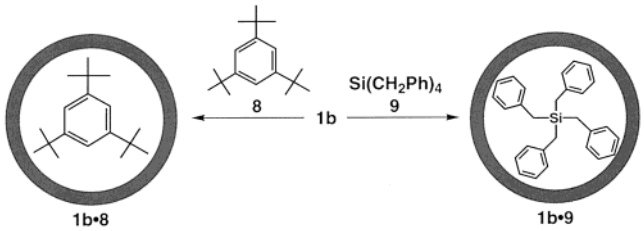

packed orthogonally, and each of them adopted a twisted conformation with a dihedral angle (ψ) of 80.6°−80.8° between two carbonyls.

For empty **1b** and **1b**·**7a** complexes, DSC analysis was carried in the range from 0 to 220 °C. For empty **1b**, only one endothermic peak appered at 134 °C, which can be assigned as the loss of water of crystallization. In addtion to this peak, two small endothermic peaks were observed at 131 and 172 °C. We could assume that these two peaks are attributed to the conformational melting of the included guest: e.g., P/M flipping of each guest molecule and fixation/unfixation of the guest dimer in the cavity.

Enclathration of Guest Molecules that are Larger than the Portals of the Cage: 1:1 Complexation. We wondered whether the cage can accommodate guest molecules that are smaller than the cavity but larger than the portals of the cage. To address this question, tri-*tert*-butylbenzene (**8**), which is slightly larger than the portal of **1b**, was examined. We found that this guest was very slowly encapsulated by the cage (Scheme 4), probably via thermally induced slippage.[8] It took over 3 h at 80 °C to obtain the 1:1 complex **1b**·**8** in ca. 45% yield ($\Delta\delta$ for *t*-Bu, −1.3; for Ar*H*, −2.3). At room temperature, enclathration and declathration were hardly observed. Hence, guest **8**, once enclathrated at elevated temperature, was not able to go out from the cavity at room temperature in a laboratory time scale, even if the solution was treated with an organic solvent.

(8) Preliminary results for **1a** were communicated in ref 5b.

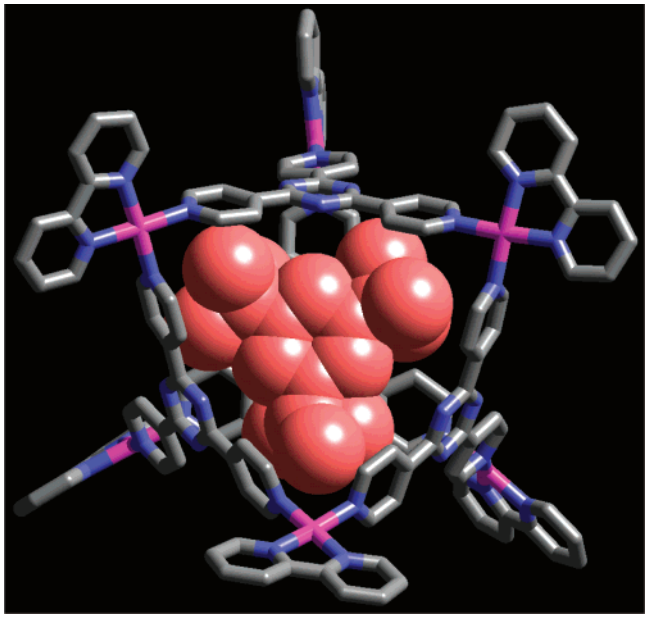

Figure 8. Crystal structure of **1b**·**8**.

After the enclathration, the solubility of **1b**·**8** becomes lower than that of free **1b**. Thus, only the **1b**·**8** complex was crystallized from the solution (Figure 8). In the crystal structure, the guest molecule was disordered and triply located with 0.33 occupancy for each, although only one of them is shown in Figure 8. The crystal structure of the **1b**·**8** complex showed that the benzene ring of the guest was located on the triazine ring of one ligand with ca. 4.5 Å face to face distance.

Tetrabenzylsilane (9). This large but conformationally flexible guest was also quantitatively enclathrated in **1b** in a 1:1 ratio (Scheme 4). Again, the complexation was very slow. Upon treating **9** with **1b** (D_2O solution), we first observed uncharacterized signals that were presumably attributed to partially recognized intermediates. Within 2 h, all of the signals were converted into a simple component that was assigned as **1b**·**9** complex. The 1:1 complexation was confirmed by X-ray crystallography. The crystal structure of **1b**·**9** showed that each portal accommodated one phenyl group of **9** (Figure 9). Though the guest adopted S_4 conformation in the solid state, the cage still kept the T_d symmetry. The conformation of **9** should be flexible, making apparent T_d symmetry in solution.

Conclusions

Newly designed cage complex **1b**, with rigid a 4,4′-bipy end-capped ligand on the Pd center, is suitable for the X-ray study of the enclathration geometry of guest molecules in the cage because of the relatively facile crystallization of the host−guest complex. Like ethylenediamine end-capped **1a**, **1b** binds various neutral organic molecules in an aqueous phase. There have been three observed enclathration modes that are controlled by the shape and size of guest molecules: (i) For more or less spherical guests, 1:4 host−guest complexation is observed where four guests from tetrahedral aggregate in the cavity. The dimension of guest molecule should be smaller than the portal size of **1b** (diameter of guest, ∼6−8 Å). (ii) For medium sized, twisteded (or bending) guests, 1:2 complexes are formed where two guest molecules are oriented orthogonally making a stable hydrophobic dimer. (iii) For larger guests with dimensions >8 Å, the

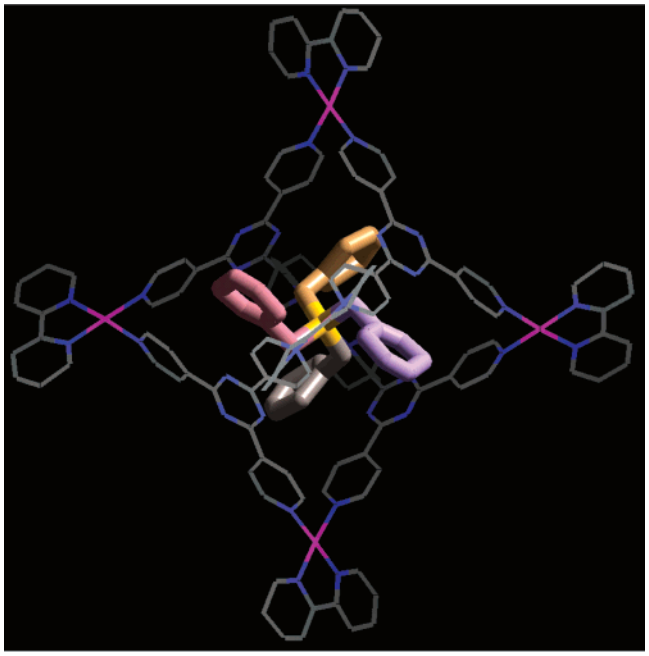

Figure 9. Crystal structure of **1b·9**.

guest molecules are enclathrated in a 1:1 ratio. These enclathration modes were confirmed by X-ray crystallography, by using 2,2′-bipy ancillary ligand which improved the crystallity of host−guest complexes.

The detailed analysis of the inclusion geometry of the molecular aggregate in the cage is expected to lead to the discovery of new physical and chemical properties in the restricted cavity of the cage. We are, in fact, developing the stabilization of otherwise labile molecules, activation of otherwise unreactive molecules, and new chemical reactions which are termed as "cavity-directed synthesis".[9]

Experimental Section

General. Melting points were determined on a Yanaco micro melting point apparatus and are uncorrected. ^{1}H NMR and ^{13}C NMR spectra were recorded on Bruker DRX-500 (500 and 125 MHz) spectrometer. FT-IR spectra were recorded on a SHIMADZU FTIR-8300 spectrometer. Mass spectra were performed on a SHIMADZU QP-5050A mass spectrometer. Elemental analyses were carried out by chemical analysis center of school of engineering Nagoya University. Column chromatography was performed with Silica Gel 60 (Merck, Art. 7734).

Synthesis of Coordination Nanocage (1b). To a solution of Pd(bipy)$(ONO_2)_2$[10] (1.00 g, 2.59 mmol) in H_2O−MeOH mixed solvents (30 mL and 30 mL) was added 2,4,6-tri(4-pyridyl)-1,3,5-triazine[11] (5.37×10^{-1} g, 1.72 mmol). The obtained suspension was stirred at 80 °C for 0.5 h. A trace amount of insoluble material was filtrated, and the clear yellow solution was evaporated to give 1.07 g (70%) of **1b** as a pale yellow crystals: mp > 300 °C (dec); ^{1}H NMR (500 MHz, D_2O, TMS as external standard) δ 9.47 (d, 24H, PyH^{α}), 8.92 (d, 24H, PyH^{β}), 8.50 (d, 12H, bipy), 8.39 (t, 12H, bipy), 7.71 (d, 12H, bipy), 7.61 (t, 12H, bipy); ^{13}C NMR (125 MHz, D_2O, $CDCl_3$ as external standard) δ 169.6 (s, triazine), 156.7 (s, bipy), 152.3 (d, PyC^{α}), 150.2 (d, bipy), 146.3 (s, triazine), 142.9 (d, bipy), 128.1 (d, bipy), 126.6 (d, PyC^{β}), 124.4 (d, bipy). Anal. Calcd for $C_{132}H_{96}N_{48}O_{36}Pd_6 \cdot 9H_2O$: C, 42.49; H, 3.08; N, 18.02. Found: C, 42.61; H, 2.81; N, 18.13.

Enclathration of *o*-Carborane (4)—A Typical Procedure. A suspension of *o*-carborane (51 μmol, 4.5 equiv.) in hexane (1 mL) was stirred with a solution of **1b** in D_2O (7.5 mM, 1.5 mL) at 25 °C for 0.5 h. The two phases were then separated. Analysis of the aqueous phase by NMR spectroscopy showed the formation of the enclathrated complex. The aqueous solution was condensed to give the enclathrated complex as a pale yellow powder.

1b·(4)$_4$ Complex: 38.9 mg of pale yellow solid, 84%; mp > 300 °C (dec); ^{1}H NMR (500 MHz, D_2O, TMS as external standard) δ 9.63 (d, 24H, PyH^{α}), 9.10 (d, 24H, PyH^{β}), 8.49 (d, 12H, bipy), 8.38 (t, 12H, bipy), 7.59 (brs, 24H, bipy), 3.81 (s, 8H, C*H* carborane), 1.8−0.0 (m, 48H, B*H* carborane); ^{13}C NMR (125 MHz, D_2O, $CDCl_3$ as external standard) δ 169.3 (s, triazine), 156.8 (s, bipy), 152.4 (d, PyC^{α}), 150.0 (d, bipy), 145.6 (s, triazine), 142.9 (d, bipy), 128.2 (d, bipy), 127.1 (d, PyC^{β}), 124.5 (d, bipy), 55.0 (d, *C*H carborane). Anal. Calcd for $C_{140}H_{144}N_{48}O_{36}B_{40}Pd_6 \cdot 4H_2O$: C, 39.87; H, 3.63; N, 15.94. Found: C, 39.53; H, 3.40; N, 16.22.

1b·(5)$_4$ Complex: The enclathrated complex was obtained in a similar manner; ^{1}H NMR (500 MHz, D_2O, TMS as external standard) δ 9.69 (d, 24H, PyH^{α}), 9.13 (d, 24H, PyH^{β}), 8.48 (d, 12H, bipy), 8.38 (t, 12H, bipy), 7.6−7.5 (m, 24H, bipy), 1.35 (brs, 24H, adamantanol), 0.2−0.4 (br, 24H, adamantanol), −0.43 (br, 12H, adamantanol); ^{13}C NMR (125 MHz, D_2O, $CDCl_3$ as external standard) δ 169.4 (s, triazine), 156.8 (s, bipy), 152.9 (d, PyC^{α}), 150.1 (d, bipy), 145.1 (s, triazine), 143.0 (d, bipy), 128.2 (d, bipy), 126.7 (d, PyC^{β}), 124.5 (d, bipy), 67.0 (s, adamantanol), 43.8 (t, adamantanol), 35.3 (t, adamantanol), 29.9 (d, adamantanol). Although NMR and X-ray analysis showed 1:4 complexation, elemental analysis suggested a part of the guest was dissociated during our attempt to isolate the complex as a pure form. For this reason, this and following complexes (**1b·(6)$_2$**, **1b·8**, **1b·9**) were not purified.

1b·(6)$_2$ Complex: ^{1}H NMR (500 MHz, D_2O, TMS as external standard) δ 9.58 (d, 24H, PyH^{α}), 8.85 (d, 24H, PyH^{β}), 8.47 (d, 12H, bipy), 8.37 (t, 12H, bipy), 7.71 (d, 12H, bipy), 7.57 (t, 12H, bipy), 5.34 (t, 8H, diphenylmethane), 4.7 (t, 8H, diphenylmethane, overlapping with H_2O signal), 4.19 (t, 4H, diphenylmethane), 1.23 (s, 4H, CH_2 diphenylmethane); ^{13}C NMR (125 MHz, D_2O, $CDCl_3$ as external standard) δ 168.9 (s, triazine), 156.7 (s, bipy), 152.6 (d, PyC^{α}), 150.3 (d, bipy), 146.0 (s, triazine), 142.9 (d, bipy), 138.8 (s, diphenylmethane), 128.2 (d, bipy), 127.6 (d, diphenylmethane), 126.9 (d, diphenylmethane), 126.5 (d, PyC^{β}), 124.4 (d, bipy), 123.7 (d, diphenylmethane), 39.7 (t, *C*H$_2$ diphenylmethane).

1b·(7a)$_2$ Complex: 44.5 mg of pale yellow solid, 97%; mp > 300 °C (dec); ^{1}H NMR (500 MHz, D_2O, TMS as external standard) δ 9.78 (d, 4H, PyH^{α}), 9.74 (d, 4H, PyH^{α}), 9.74 (d, 4H, PyH^{α}), 9.61 (d, 4H, PyH^{α}), 9.36 (d, 4H, PyH^{α}), 9.18 (d, 4H, PyH^{β}), 9.08 (d, 4H, PyH^{β}), 9.05 (d, 4H, PyH^{β}), 8.93 (d, 4H, PyH^{β}), 8.61 (d, 4H, PyH^{β}), 8.50 (t, 12H, bipy), 8.40 (t, 12H, bipy), 8.37 (d, 4H, PyH^{β}), 7.7−7.5 (m, 28H, 24H for bipy, 4H for diketone Ar*H*), 5.66 (d, 4H, diketone Ar*H*), 4.05 (d, 4H, diketone Ar*H*), 3.52 (d, 4H, diketone Ar*H*), 2.80 (s, 12H, diketone CH_3O^-); ^{13}C NMR (125 MHz, D_2O, $CDCl_3$ as external standard) δ 193.0 (s, diketone *C*O), 169.6 (s, triazine), 169.5 (s, triazine), 169.3 (s, triazine), 163.0 (s, diketone), 157.14 (s, bipy), 157.08 (s, bipy), 153.5 (d, Py), 153.3 (d, Py), 153.2 (d, Py), 153.0 (d, Py), 152.9 (d, Py), 152.8 (d, Py), 150.6 (d, bipy), 150.4 (d, Py), 150.3 (d, Py), 146.3 (s, Py), 145.3 (s, Py), 145.0 (s, Py), 143.3 (d, bipy), 143.2 (d, bipy), 132.3 (d, diketone Ar), 132.3 (d, diketone Ar), 129.7 (d, diketone Ar), 128.5 (d, Py, bipy), 127.8 (d, Py), 127.6 (d, Py), 126.5 (d, Py), 126.2 (d, Py), 124.9 (d, bipy), 124.8 (d, bipy), 124.1 (s, diketone Ar), 120.4 (s, diketone Ar), 107.4 (d, diketone Ar), 56.5 (q, diketone *C*H$_3$O$^-$); IR (KBr) 1656 cm^{-1}. Anal. Calcd for $C_{164}H_{124}N_{48}O_{44}Pd_6 \cdot 10H_2O$: C, 45.92; H, 3.38; N, 15.67. Found: C, 45.71; H, 3.21; N, 15.58.

(9) (a) Ito, H.; Kusukawa, T.; Fujita, M. *Chem. Lett.* **2000**, 598. (b) Yoshizawa, M.; Kusukawa, T.; Fujita, M.; Yamaguchi, K. *J. Am. Chem. Soc.* **2000**, *122*, 6311. (c) Yoshizawa, M.; Kusukawa, T.; Fujita, M.; Sakamoto, S.; Yamaguchi, K. *J. Am. Chem. Soc.* **2001**, *123* 10454. (d) Yoshizawa, M.; Takeyama, Y.; Kusukawa, T.; Fujita, M. *Angew. Chem., Int. Ed.* **2002**, *41*, 1347.

(10) Wimmer, S.; Castan, P.; Wimmer, F. L.; Johnson, N. P. *J. Chem. Soc., Dalton Trans.* **1989**, 403.

(11) Anderson, L. H.; Anderson, S.; Sanders, M. K. *J. Chem. Soc., Perkin Trans. 1.* **1995**, 2231.

1b·(7b)$_2$ Complex: 43.1 mg of pale yellow solid, 93%; mp > 300 °C (dec); ^{1}H NMR (500 MHz, D_2O, TMS as external standard) δ 9.8−9.6 (m, 20H, PyH^{α}), 9.45 (t, 2H, PyH^{α}), 9.37 (t, 2H, PyH^{α}), 9.2−8.0 (m, 20H, PyH^{β}), 8.51 (t, 14H, 12H for bipy, 2H for PyH^{β}), 8.4 (m, 14H, 12H for bipy, 2H for PyH^{β}), 7.8−7.4 (m, 28H, 24H for bipy, 4H for diketone Ar*H*), 5.75 (d, 1H, diketone Ar*H*), 5.68 (d, 1H, diketone Ar*H*), 5.25 (t, 1H, diketone Ar*H*), 5.18 (d, 1H, diketone Ar*H*), 4.1−3.9 (m, 4H, diketone Ar*H*), 3.6−3.4 (m, 4H, diketone Ar*H*), 3.3−2.8 (m, 4H, diketone CH_2), 2.81 (s, 3H, diketone CH_3O), 2.78 (s, 3H, diketone CH_3O), 1.21 (t, J = 6.9 Hz, 3H, diketone CH_3CH$_2$), 1.10 (t, J = 7.0 Hz, 3H, diketone CH_3CH$_2$); IR (KBr) 1660 cm^{-1}. Anal. Calcd for $C_{166}H_{128}N_{48}O_{44}Pd_6$·12$H_2O$: C, 45.79; H, 3.52; N, 15.44. Found: C, 45.70; H, 3.44; N, 15.43.

1b·8 Complex: ^{1}H NMR (500 MHz, D_2O, TMS as external standard) δ 9.58 (br, 24H, PyH^{α}), 8.97 (br, 24H, PyH^{β}), 8.48 (d, 12H, bipy), 8.38 (t, 12H, bipy), 7.77 (d, 12H, bipy), 7.59 (t, 12H, bipy), 4.98 (s, 3H, Ar*H* *tert*-butylbenzene), 0.04 (s, 27H, *t*-Bu); ^{13}C NMR (125 MHz, D_2O, $CDCl_3$ as external standard) δ 169.3 (s, triazine), 156.7 (s, bipy), 152.7 (d, PyC^{α}), 150.4 (d, bipy), 149.0 (s, *tert*-butylbenzene), 145.4 (s, triazine), 143.0 (d, bipy), 128.2 (d, bipy), 126.4 (d, PyC^{β}), 124.4 (d, bipy), 116.3 (d, Ar *tert*-butylbenzene), 33.3(s, *t*-Bu), 25.5(q, *t*-Bu).

1b·9 Complex: ^{1}H NMR (500 MHz, D_2O, TMS as external standard) δ 9.61 (d, 24H, PyH^{α}), 8.85 (d, 24H, PyH^{β}), 8.52 (d, 12H, bipy), 8.42 (t, 12H, bipy), 7.79 (d, 12H, bipy), 7.62 (t, 12H, bipy), 7.09 (t, 4H, tetrabenzylsilane), 6.62 (t, 8H, tetrabenzylsilane), 4.7 (d, 8H, tetrabenzylsilane overlapping with H_2O signal), −0.13 (s, 8H, CH_2 tetrabenzylsilane); ^{13}C NMR (125 MHz, D_2O, $CDCl_3$ as external standard) δ 169.3 (s, triazine), 156.7 (s, bipy), 152.7 (d, PyC^{α}), 150.4 (d, bipy), 145.5 (s, triazine), 143.0 (d, bipy), 136.0 (s, tetrabenzylsilane), 128.2 (d, bipy and d, tetrabenzylsilane), 126.6 (d, tetrabenzylsilane), 126.3 (d, PyC^{β}), 125.2 (d, tetrabenzylsilane), 124.5 (d, bipy), 18.6 (t, *C*H_2 tetrabenzylsilane).

Crystallographic Analysis. Crystals suitable for X-ray analysis of the following dimensions were prepared to stand at ambient temperature for a few days: 0.40 × 0.40 × 0.50 mm for **1b·(4)**$_4$, 0.30 × 0.30 × 0.40 mm for **1b·(5)**$_4$, 0.20 × 0.20 × 0.30 mm for **1b·(6)**$_2$, 0.50 × 0.50 × 0.50 mm for **1b·(7a)**$_2$, 0.10 × 0.10 × 0.40 mm for **1b·8**, 0.40 × 0.40 × 0.50 mm for **1b·9**. Diffraction measurements were made on a Bruker SMART CCD diffractometer. In all cases, very precise refinement was unsuccessful because of the high degree of disorder of the counterions and water molecules.

1b·(4)$_4$ Complex: $C_{140}H_{144}N_{48}O_{36}B_{40}Pd_6$·($H_2O$)$_{29}$, M = 4668.30, tetragonal space group $P4_12_12$ (no. 92), $a = b$ = 29.146(3) Å, c = 30.712(5) Å, V = 260 90(6) Å^3, Z = 4, ρ_{calcd} = 1.188 g/cm^3, F(000) = 9496, radiation, λ(Mo$_{K\alpha}$) = 0.71073 Å, T = 123 K, reflections collected/unique 84 388/11823 (R_{int} = 0.0834). The structure was solved by direct methods (SHELXL-97) and refined by full-matrix least-squares methods on F^2 with 1210 parameters. $R1$ = 0.0927 ($I > 2\sigma(I)$), $wR2$ = 0.2274, GOF 1.932; max./min. residual density 0.875/−0.461 eÅ^{-3}.

1b·(5)$_4$ Complex: $C_{172}H_{160}N_{48}O_{40}Pd_6$·($H_2O$)$_{29}$, M = 4700.34, tetragonal space group $P4_32_12$ (no. 96), $a = b$ = 29.189(4) Å, c = 30.337-(6) Å, V = 25847(7) Å^3, Z = 4, ρ_{calcd} = 1.208 g/cm^3, F(000) = 9656, radiation, λ(Mo$_{K\alpha}$) = 0.710 73 Å, T = 118 K, reflections collected/unique 87737/13515 (R_{int} = 0.0962). The structure was solved by direct methods (SHELXL-97) and refined by full-matrix least-squares methods on F^2 with 1087 parameters. $R1$ = 0.1038 ($I > 2\sigma(I)$), $wR2$ = 0.2462, GOF 2.096; max./min. residual density 1.524/−0.819 eÅ^{-3}.

1b·(6a)$_2$ Complex: $C_{158}H_{182}N_{48}O_{67}Pd_6$·($H_2O$)$_{31}$, M = 4463.92, tetragonal space group $P4_12_12$ (no. 92), $a = b$ = 30.4810(14) Å, c = 28.842 3(19) Å, V = 26797(2) Å^3, Z = 4, ρ_{calcd} = 1.106 g/cm^3, F(000) = 9112, radiation, λ(Mo$_{K\alpha}$) = 0.710 73 Å, T = 123 K, reflections collected/unique 174196/30829 (R_{int} = 0.1032). The structure was solved by direct methods (SHELXL-97) and refined by full-matrix least-squares methods on F^2 with 1147 parameters. R_1 = 0.0829 ($I > 2\sigma$-(I)), wR_2 = 0.2124, GOF 1.461; max./min. residual density 1.582/−0.713 eÅ^{-3}.

1b·(7)$_2$ Complex: $C_{164}H_{124}N_{48}O_{44}Pd_6$, M = 4109.51, tetragonal space group $P4_32_12$ (no. 96), $a = b$ = 29.535(3), c = 31.351(4) Å, V = 27349(5) Å^3, Z = 4, ρ_{calcd} = 0.998 g/cm^3, F(000) = 8288, radiation, λ(Mo$_{K\alpha}$) = 0.71073 Å, T = 298 K, reflections collected/unique 88739/12358 (R_{int} = 0.0615). The structure was solved by direct methods (SHELXL-97) and refined by full-matrix least-squares methods on F^2 with 865 parameters. R_1 = 0.1080 ($I > 2\sigma(I)$), wR_2 = 0.2809, GOF 2.151; max./min. residual density 1.000/−0.655 eÅ^{-3}.

1b·8 Complex: $C_{150}H_{126}N_{48}O_{36}Pd_6$·($H_2O$)$_{10}$, M = 3995.55, trigonal space group *P*-3*c1* (no. 165), $a = b$ = 28.080 (19) Å, c = 34.09(3) Å, V = 23282(31) Å^3, Z = 4, ρ_{calcd} = 1.140 g/cm^3, F(000) = 8104, radiation, λ(Mo$_{K\alpha}$) = 0.71073 Å, T = 153 K, reflections collected/unique 123461/17806 (R_{int} = 0.0627). The structure was solved by direct methods (SHELXL-97) and refined by full-matrix least-squares methods on F^2 with 823 parameters. R_1 = 0.0709 ($I > 2\sigma(I)$), wR_2 = 0.2055, GOF 1.491; max./min. residual density 1.068/−1.178 eÅ^{-3}.

1b·9 Complex: $C_{160}H_{124}N_{48}O_{36}Pd_6Si$·($H_2O$)$_{22}$, M = 4357.91, tetragonal space group $P4_32_12$ (no. 96), $a = b$ = 29.0082(8), c = 29.7539-(12) Å, V = 25037.2(14) Å^3, Z = 4, ρ_{calcd} = 1.156 g/cm^3, F(000) = 8872, radiation, λ(Mo$_{K\alpha}$) = 0.71073 Å, T = 118 K, reflections collected/unique 162275/28779 (R_{int} = 0.0678). The structure was solved by direct methods (SHELXL-97) and refined by full-matrix least-squares methods on F^2 with 865 parameters. R_1 = 0.0969 ($I > 2\sigma(I)$), wR_2 = 0.2512, GOF 1.445; max./min. residual density 0.895/−0.681 eÅ^{-3}.

Supporting Information Available: X-ray crystallographic details and NMR data for complexes **1b·(4)**$_4$, **1b·(5)**$_4$, **1b·(6)**$_2$, **1b·(7a)**$_2$, **1b·(7b)**$_2$, **1b·8**, and **1b·9** (PDF). This material is available free of charge via the Internet at http://pubs.acs.org.

JA020712K